Cell Reports, Volume *17*

Supplemental Information

Lsd1 Ablation Triggers Metabolic Reprogramming of Brown Adipose Tissue

Delphine Duteil, Milica Tosic, Franziska Lausecker, Hatice Z. Nenseth, Judith M. Müller, Sylvia Urban, Dominica Willmann, Kerstin Petroll, Nadia Messaddeq, Laura Arrigoni, Thomas Manke, Jan-Wilhelm Kornfeld, Jens C. Brüning, Vyacheslav Zagoriy, Michael Meret, Jörn Dengjel, Toufike Kanouni, and Roland Schüle

Supplemental Informations

Lsd1 ablation triggers metabolic reprogramming of brown adipose tissue

Delphine Duteil, Milica Tosic, Franziska Lausecker, Hatice Z. Nenseth, Judith M. Müller, Sylvia Urban, Dominica Willmann, Kerstin Petroll, Nadia Messaddeq, Laura Arrigoni, Jan-Wilhelm Kornfeld, Jens C. Brüning, Vyacheslav Zagoriy, Michael Meret, Jörn Dengjel, Thomas Manke, and Roland Schüle

Supplemental Figures and Legends

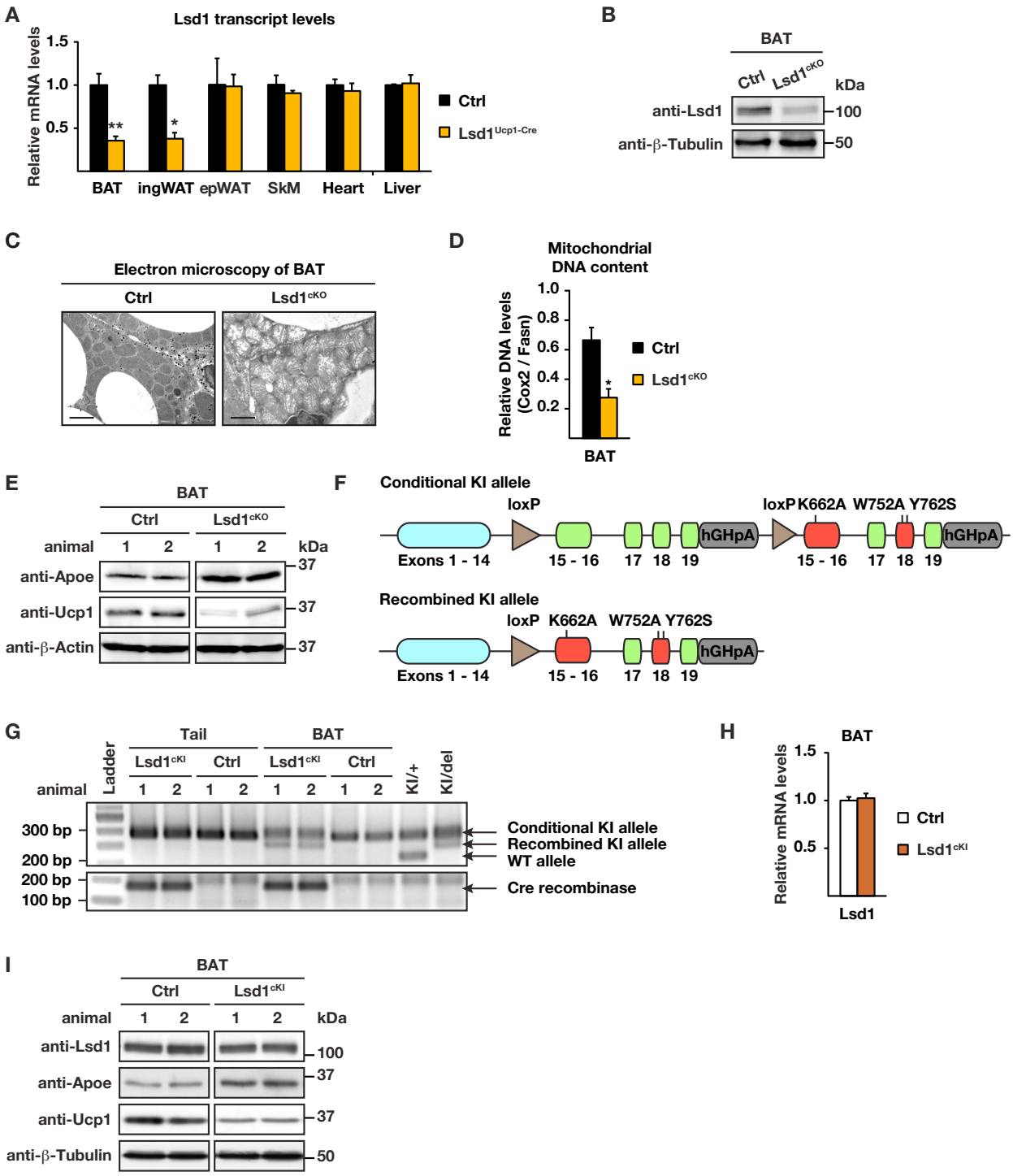

Figure S1 (related to Figure 1). Lsd1 represses the expression of WAT-selective genes in BAT.
(A) Relative Lsd1 mRNA levels in interscapular brown adipose tissue (BAT), inguinal white adipose tissue (ingWAT), epididymal white adipose tissue (epWAT), skeletal muscle (SkM), heart, and liver of control (Ctrl) and Lsd1^{cKO} mice (mean + SEM, *p<0.05, **p<0.01, Ctrl n = 9, Lsd1^{cKO} n = 7).
(B) Western blot analysis of Lsd1 in BAT of Ctrl and Lsd1^{cKO} mice. β-Tubulin was used as a loading control.
(C) Ultrastructure analysis of representative BAT sections of Ctrl and Lsd1^{cKO} mice. Scale bar: 2 µm.
(D) Ratio of mitochondria to nuclear DNA content assessed by quantitative PCR of the mitochondria-encoded Cox2 and the nuclear-encoded Fasn gene in BAT of Ctrl and Lsd1^{cKO} mice (mean + SEM, *p<0.05, n = 5).
(E) Western blot analysis of Apoe and Ucp1 in BAT of Ctrl and Lsd1^{cKO} mice. β-Actin was used as a loading control.
(F) Scheme depicting the *Lsd1* knock-in (KI) allele.
(G) Genotyping of mouse tail and BAT biopsies of Ctrl and Lsd1^{cKO} mice for the presence of Lsd1 conditional or recombined KI alleles (upper panel), or Ucp1-Cre recombinase (lower panel) by semi-quantitative PCR.
(H) Relative Lsd1 mRNA levels in BAT of Ctrl and Lsd1^{cKI} mice (mean + SEM, Ctrl n = 7, Lsd1^{cKI} n = 6).
(I) Western blot analysis of Lsd1, Apoe, and Ucp1 in BAT of Ctrl and Lsd1^{cKI} mice. β-Tubulin was used as a loading control.

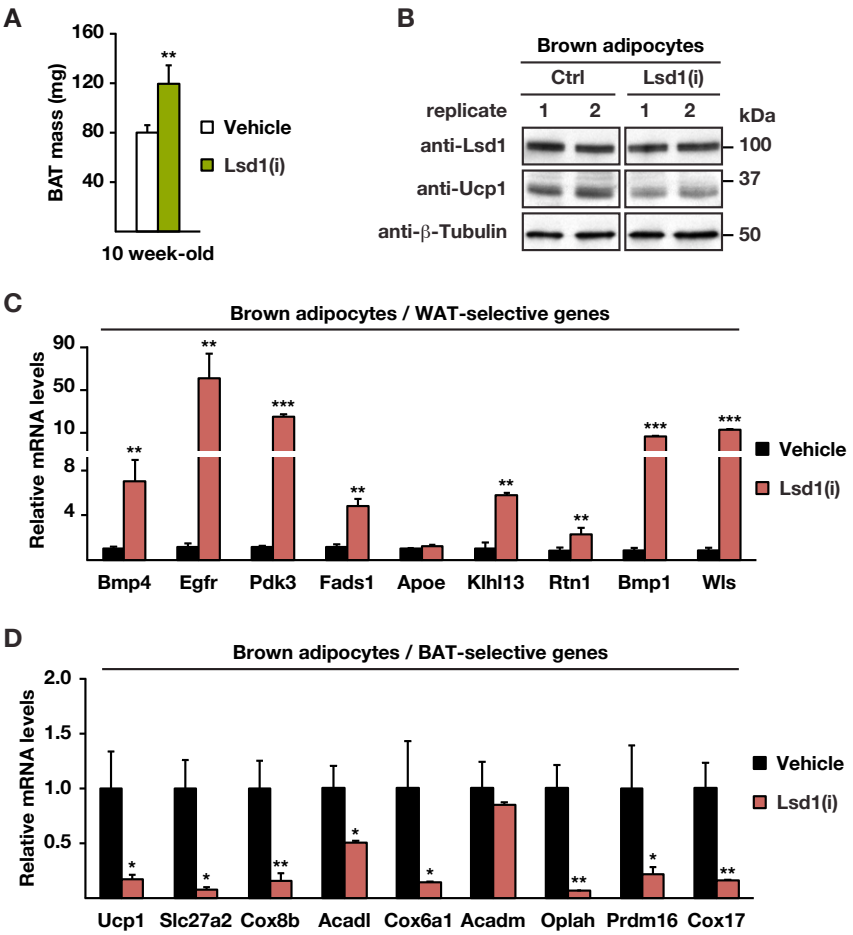

Figure S2 (related to Figure 2). The demethylase activity of Lsd1 is required to maintain BAT properties.
(A) Mass of BAT of 10 week-old mice treated with vehicle or Lsd1-specific inhibitor [Lsd1(i)] (mean + SEM, **p<0.01, vehicle n = 6, Lsd1(i) n = 7).
(B) Western blot analysis of Lsd1 and Ucp1 in brown adipocytes treated with vehicle or Lsd1(i). β-Tubulin was used as a loading control.
(C-D) Relative mRNA levels of (C) WAT- and (D) BAT-selective genes in brown adipocytes treated with vehicle or Lsd1(i) (mean + SEM, *p<0.05, **p<0.01, ***p<0.001, n = 6).

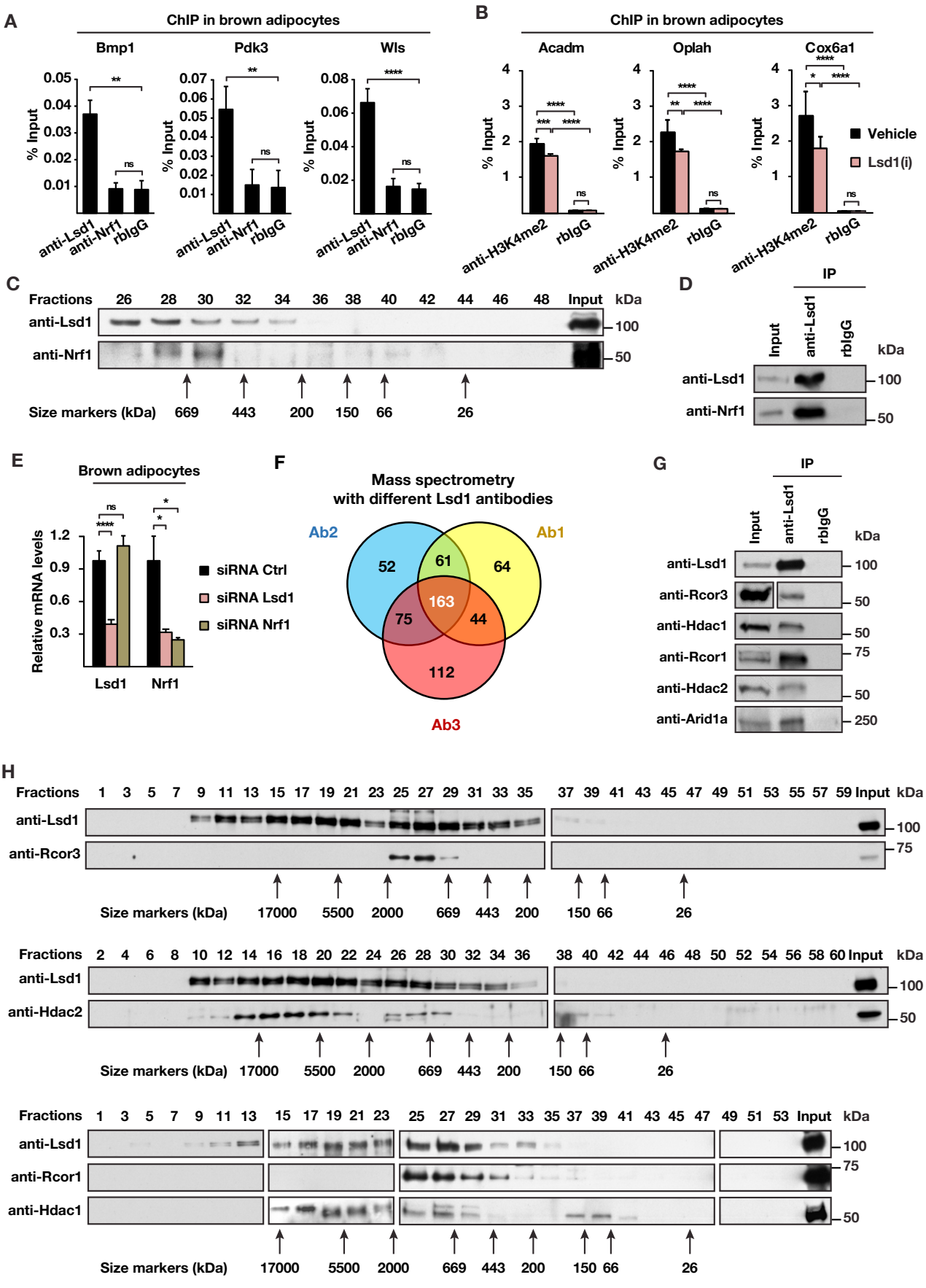
A
ChIP in brown adipocytes
Bmp1
Pdk3
Wls
% Input
anti-Lsd1
anti-Nrf1
rbIgG
B
ChIP in brown adipocytes
Acadm
Oplah
Cox6a1
anti-H3K4me2
rbIgG
Vehicle
Lsd1(i)
C
Fractions
Input
kDa
anti-Lsd1
anti-Nrf1
Size markers (kDa)
669
443
200
150
66
26
D
IP
Input
anti-Lsd1
rbIgG
E
Brown adipocytes
Relative mRNA levels
siRNA Ctrl
siRNA Lsd1
siRNA Nrf1
Lsd1
Nrf1
F
Mass spectrometry
with different Lsd1 antibodies
Ab1
Ab2
Ab3
52
61
64
163
75
44
112
G
anti-Rcor3
anti-Hdac1
anti-Rcor1
anti-Hdac2
anti-Arid1a
H
anti-Hdac1
17000
5500
2000

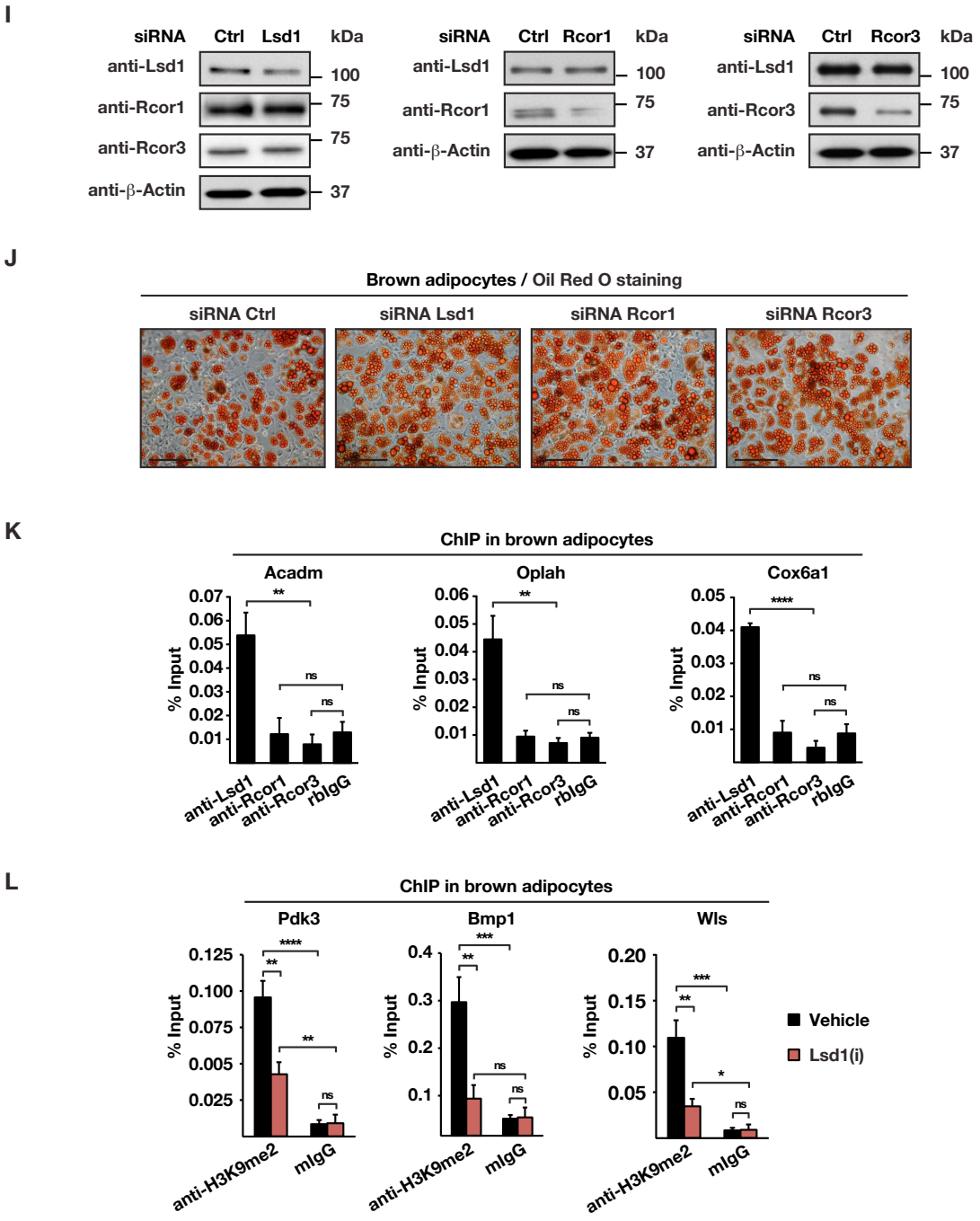

Figure S3 (related to Figure 3). Lsd1 regulates the brown fat program through a dual mechanism

(A) ChIP analysis to detect promoter occupancy performed with anti-Lsd1 and anti-Nrf1 antibodies or rabbit IgG (rbIgG) in brown adipocytes for indicated genes. The precipitated chromatin was quantified by qPCR analysis with primers flanking Lsd1-binding sites in the indicated genes (mean + SEM, n = 3).

(B) ChIP analysis to detect promoter occupancy performed with anti-H3K4me2 antibody or rbIgG in brown adipocytes treated with Lsd1(i) or vehicle. The precipitated chromatin was quantified by qPCR analysis with primers flanking Lsd1-binding sites in the indicated genes (mean + SEM, n = 3).

(C) Western blot analysis of individual fractions of brown adipocyte nuclear extracts obtained after gel filtration. Membranes were decorated with Lsd1 or Nrf1 antibody.

(D) Immunoprecipitation of Nrf1 with Lsd1 antibody from BAT nuclear extracts. Membranes were decorated with Lsd1 or Nrf1 antibody. Rabbit IgG (rbIgG) served as a control.

(E) Relative mRNA levels of Lsd1 and Nrf1 in brown adipocytes transfected with siRNA Ctrl, siRNA Lsd1, or siRNA Nrf1 (mean + SEM, n = 3). In agreement with previous data (Duteil et al., 2014), knock-down of Lsd1 results in reduced mRNA levels of Nrf1.

(F) Venn diagram depicting the overlap between Lsd1 interacting proteins identified by immunoprecipitation using three different Lsd1 antibodies followed by mass spectrometry. Ab1 and Ab2 correspond to 2 homemade anti-Lsd1 antibodies (see Experimental procedures for details) and Ab3 corresponds to the L-4481 (Sigma) anti-Lsd1 antibody.

(G) Immunoprecipitation of components of the CoREST complex with Lsd1 antibody from BAT nuclear extracts. Membranes were decorated with the indicated antibodies. Rabbit IgG (rbIgG) served used as a control.
(H) Western blot analysis of individual fractions of brown adipocyte nuclear extracts obtained after gel filtration. Membranes were decorated with the indicated antibodies.
(I) Western blot analysis of Lsd1, Rcor1, and Rcor3 in brown adipocytes transfected with siRNA Ctrl, siRNA Lsd1, siRNA Rcor1, or siRNA Rcor3. β-Tubulin was used as a loading control.
(J) Oil red O staining of brown adipocytes transfected with siRNA Ctrl, siRNA Lsd1, siRNA Rcor1, or siRNA Rcor3. Scale bar: 50 μm.
(K-L) ChIP analysis to detect promoter occupancy performed with (K) anti-Lsd1, anti-Rcor1, and anti-Rcor3 antibody or rbIgG, and (L) anti-H3K9me2 antibody or mIgG in brown adipocytes treated with Lsd1(i) or vehicle. The precipitated chromatin was quantified by qPCR analysis with primers flanking Lsd1-binding sites in the indicated genes (mean + SEM, n = 3).
(A), (E), (K): one-way ANOVA; (B), (L): two-way ANOVA; *p<0.05, **p<0.01, ***p<0.001, ****p<0.0001.

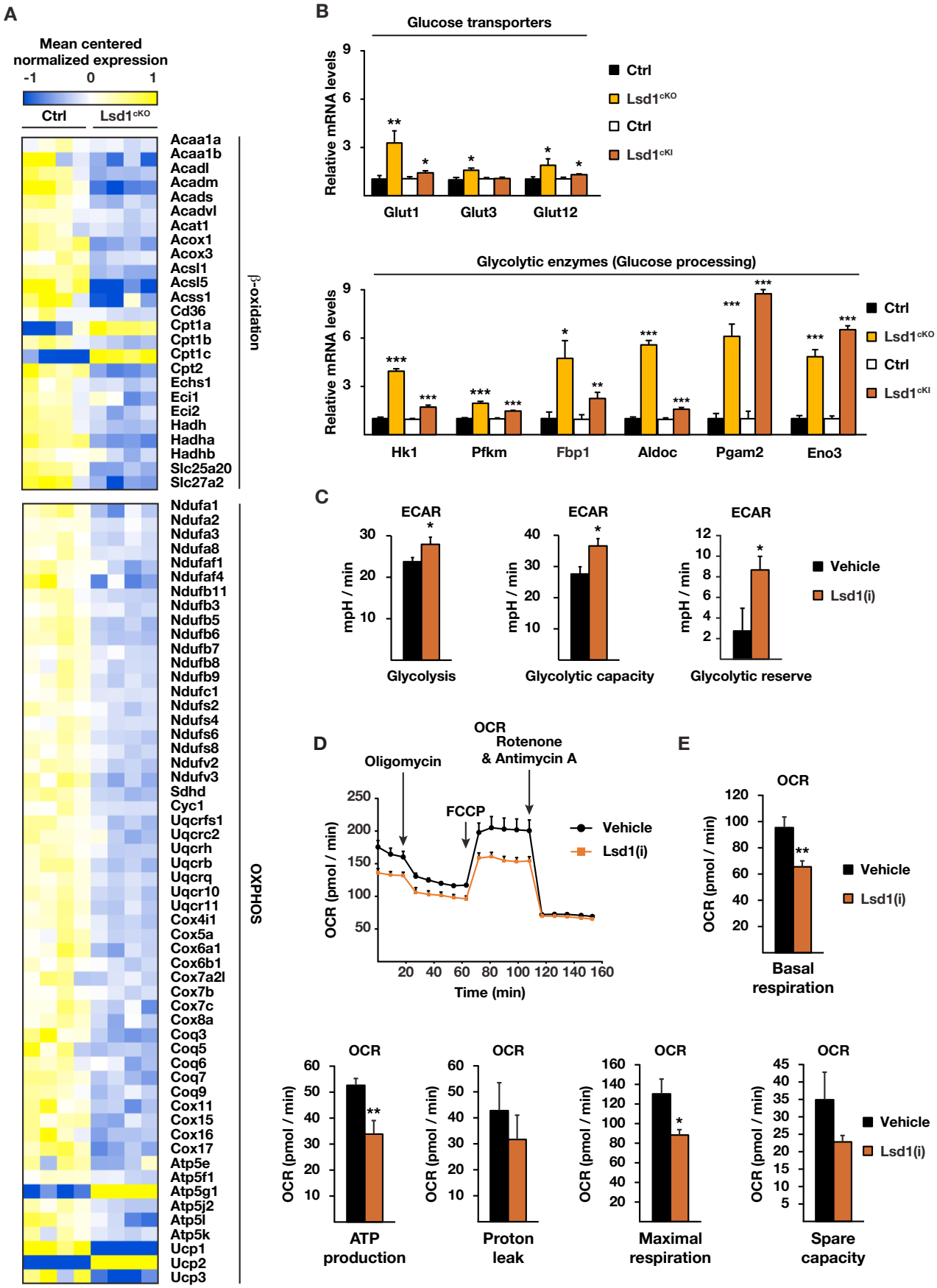
A
Mean centered normalized expression
-1
0
1
Ctrl
Lsd1cKO
Acaa1a
Acaa1b
Acadl
Acadm
Acads
Acadvl
Acat1
Acox1
Acox3
Acsl1
Acsl5
Acss1
Cd36
Cpt1a
Cpt1b
Cpt1c
Cpt2
Echs1
Eci1
Eci2
Hadh
Hadha
Hadhb
Slc25a20
Slc27a2
β-oxidation
Ndufa1
Ndufa2
Ndufa3
Ndufa8
Ndufaf1
Ndufaf4
Ndufb11
Ndufb3
Ndufb5
Ndufb6
Ndufb7
Ndufb8
Ndufb9
Ndufc1
Ndufs2
Ndufs4
Ndufs6
Ndufs8
Ndufv2
Ndufv3
Sdhd
Cyc1
Uqcrfs1
Uqcrc2
Uqcrh
Uqcrb
Uqcrq
Uqcr10
Uqcr11
Cox4i1
Cox5a
Cox6a1
Cox6b1
Cox7a2l
Cox7b
Cox7c
Cox8a
Coq3
Coq5
Coq6
Coq7
Coq9
Cox11
Cox15
Cox16
Cox17
Atp5e
Atp5f1
Atp5g1
Atp5j2
Atp5l
Atp5k
Ucp1
Ucp2
Ucp3
OXPHOS
B
Glucose transporters
Relative mRNA levels
Ctrl
Lsd1cKO
Ctrl
Lsd1cKI
Glut1
Glut3
Glut12
Glycolytic enzymes (Glucose processing)
Hk1
Pfkm
Fbp1
Aldoc
Pgam2
Eno3
C
ECAR
mpH / min
Glycolysis
Glycolytic capacity
Glycolytic reserve
Vehicle
Lsd1(i)
D
OCR
Oligomycin
Rotenone & Antimycin A
FCCP
OCR (pmol / min)
Time (min)
E
Basal respiration
ATP production
Proton leak
Maximal respiration
Spare capacity

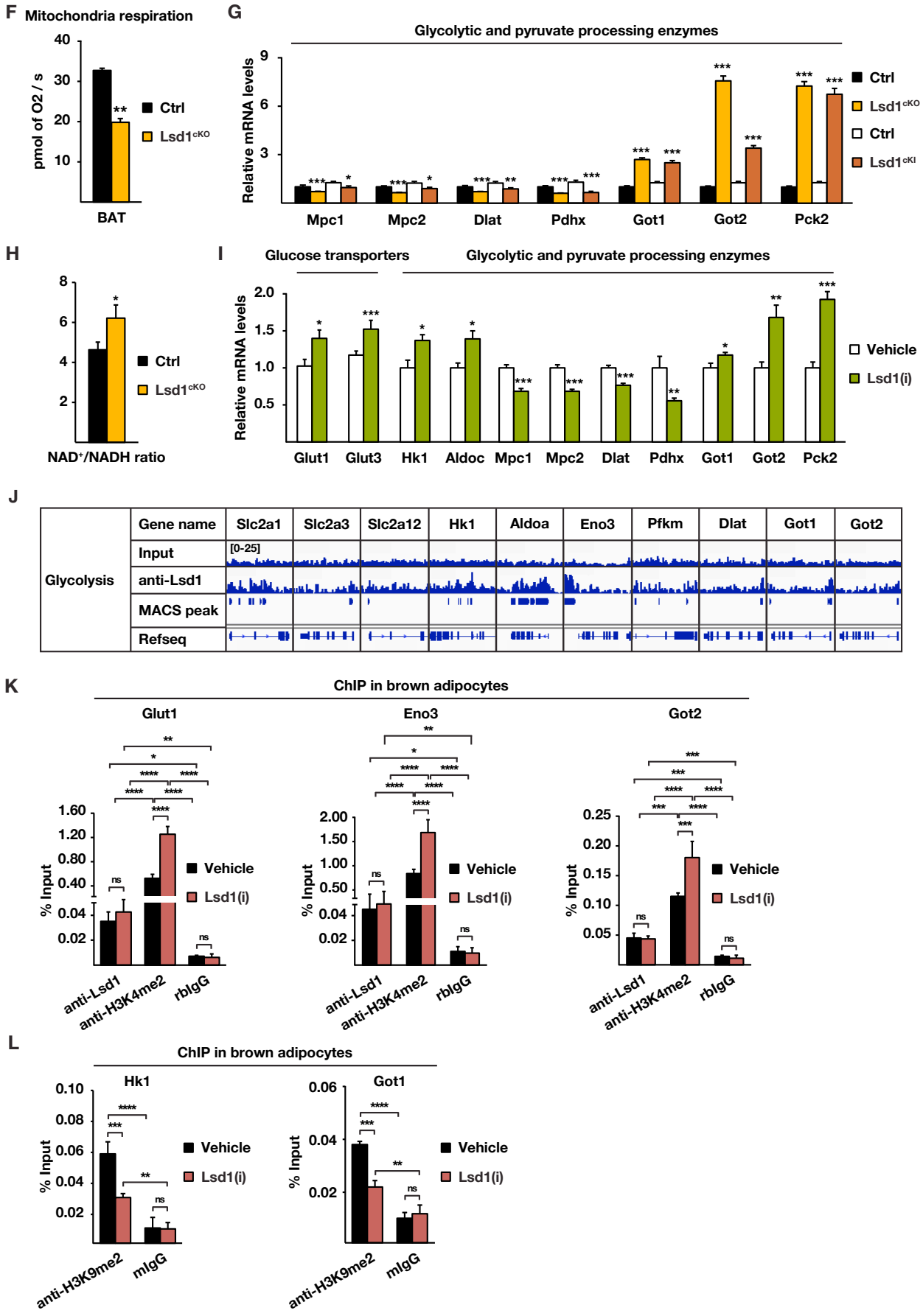

Figure S4 (related to Figure 4). Lsd1 represses glycolysis in BAT.
(A) Heatmaps depicting mRNA levels of genes involved in β-oxidation and oxidative phosphorylation (OXPHOS) in BAT of 10 week-old control (Ctrl) and Lsd1^{cKO} mice.

(B) Relative mRNA levels of genes encoding glucose transporters and glycolytic enzymes in BAT of Ctrl, Lsd1^{cKO}, and Lsd1^{cKI} mice [mean + SEM, *p<0.05, **p<0.01, ***p<0.001, Ctrl (black bars) n = 9, Lsd1^{cKO} (orange bars) n = 7, Ctrl (white bars) n = 7, and Lsd1^{cKI} (red bars) n = 6].
(C) Glycolysis, maximal glycolytic capacity and glycolytic reserve deduced from extracellular acidification rate (ECAR) (mean + SEM, *p<0.05, n = 6).
(D-E) Oxygen consumption rate (OCR) of vehicle- or Lsd1(i) treated brown adipocytes determined by the Seahorse Extracellular Flux Analyzer (mean + SEM, *p<0.05, n = 9).
(F) Mitochondrial respiration of BAT extracts from Ctrl and Lsd1^{cKO} mice assessed with a high-resolution respiratory Oxygraph-2K system (mean + SEM, **p<0.01, n = 5).
(G) Relative mRNA levels of genes encoding glycolytic and pyruvate processing enzymes in BAT of Ctrl, Lsd1^{cKO}, and Lsd1^{cKI} mice [mean + SEM, *p<0.05, **p<0.01, ***p<0.001, Ctrl (black bars) n = 9, Lsd1^{cKO} (orange bars) n = 7, Ctrl (white bars) n = 7, and Lsd1^{cKI} (red bars) n = 6].
(H) Determination of the NAD^+/NADH ratio in BAT of Ctrl and Lsd1^{cKO} mice at 10 weeks of age (mean + SEM, **p<0.01, ***p<0.001, n = 6).
(I) Relative mRNA levels of selected genes encoding glucose transporters, glycolytic, and pyruvate processing enzymes in BAT of mice treated with vehicle or Lsd1(i) [mean + SEM, *p<0.05, **p<0.01, ***p<0.001, Vehicle n = 6, Lsd1(i) n = 7].
(J) Localization of Lsd1 at the promoter of representative genes encoding glucose transporters, glycolytic and pyruvate processing enzymes in brown adipocytes.
(K-L) ChIP analysis to detect promoter occupancy performed with (K) anti-Lsd1 and anti-H3K4me2 antibody, or rbIgG or (L) anti-H3K9me2 antibody, or mIgG in brown adipocytes treated with vehicle or Lsd1(i). The precipitated chromatin was quantified by qPCR analysis with primers flanking Lsd1-binding sites in the indicated genes (mean + SEM, two-way ANOVA, ns: p>0.05, *p<0.05, **p<0.01, ***p<0.001, ****p<0.0001, n = 3).

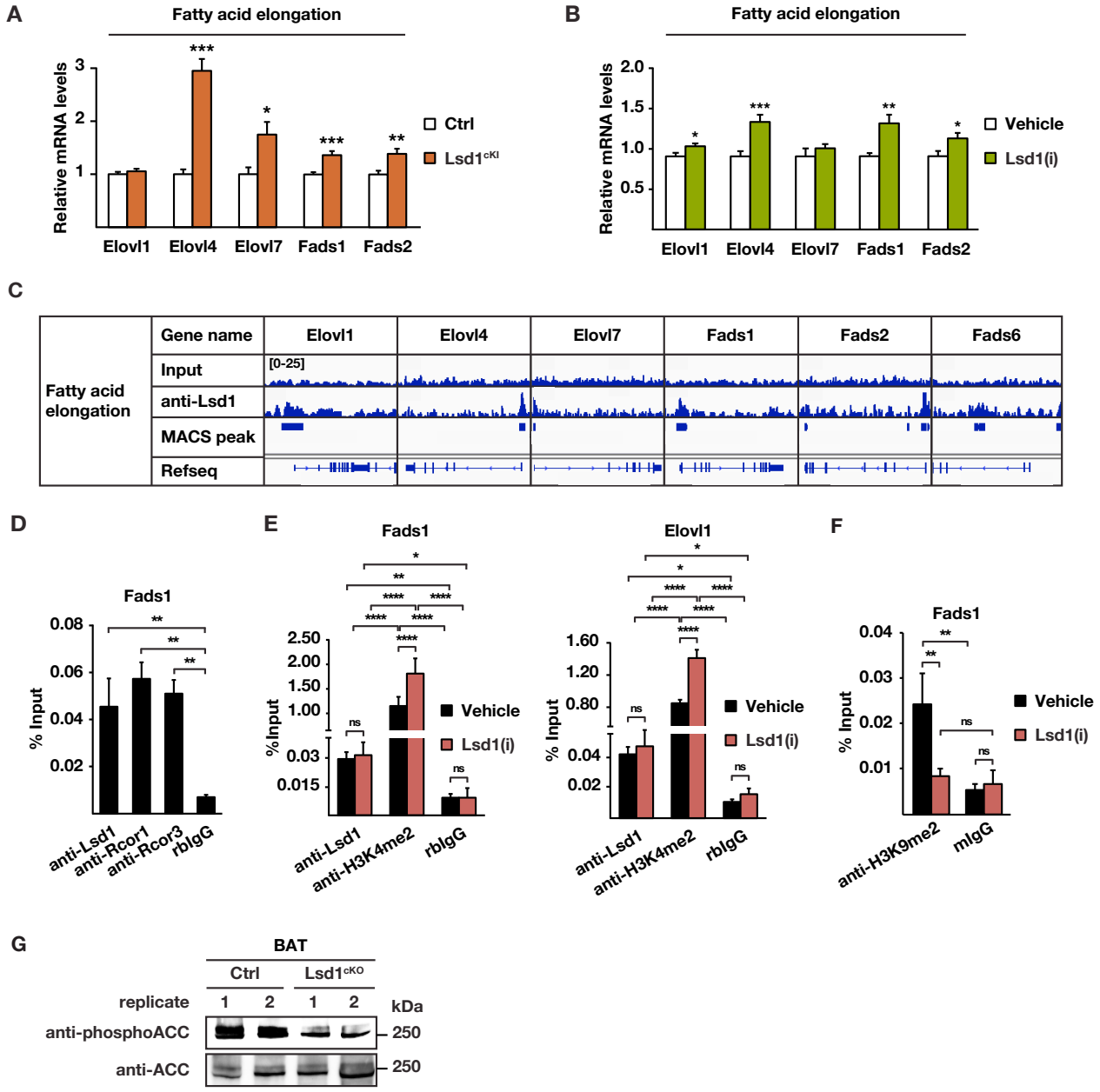

Figure S5 (related to Figure 5). Lsd1 limits fat accumulation in BAT.
(A-B) Relative mRNA levels of indicated enzymes involved in fatty acid elongation in BAT of (A) Ctrl and Lsd1^{cKI} mice and (B) mice treated with vehicle or Lsd1(i) [(A-B) mean + SEM, *p<0.05, **p<0.01, ***p<0.001; (A) Ctrl n = 7, Lsd1^{cKI} n = 6; (B) Vehicle n = 6, Lsd1(i) n = 7].
(C) Localization of Lsd1 at the promoter of representative genes encoding enzymes involved in fatty acid elongation in brown adipocytes.
(D-F) ChIP analysis to detect promoter occupancy performed with with (D) anti-Lsd1, anti-Rcor1, and anti-Rcor3 antibody or rbIgG in brown adipocytes, (E) anti-Lsd1 and anti-H3K4me2 antibody, or rbIgG, or (F) anti-H3K9me2 antibody, or mIgG in brown adipocytes treated with vehicle or Lsd1(i). The precipitated chromatin was quantified by qPCR analysis with primers flanking Lsd1-binding sites in the indicated genes (mean + SEM, (D) one-way ANOVA, (E-F) two-way ANOVA, ns: p>0.05, *p<0.05, **p<0.01, ***p<0.001, ****p<0.0001, n = 3).
(G) Western blot analysis of phosphor-ACC and total ACC in BAT of Ctrl and Lsd1^{cKO} mice.

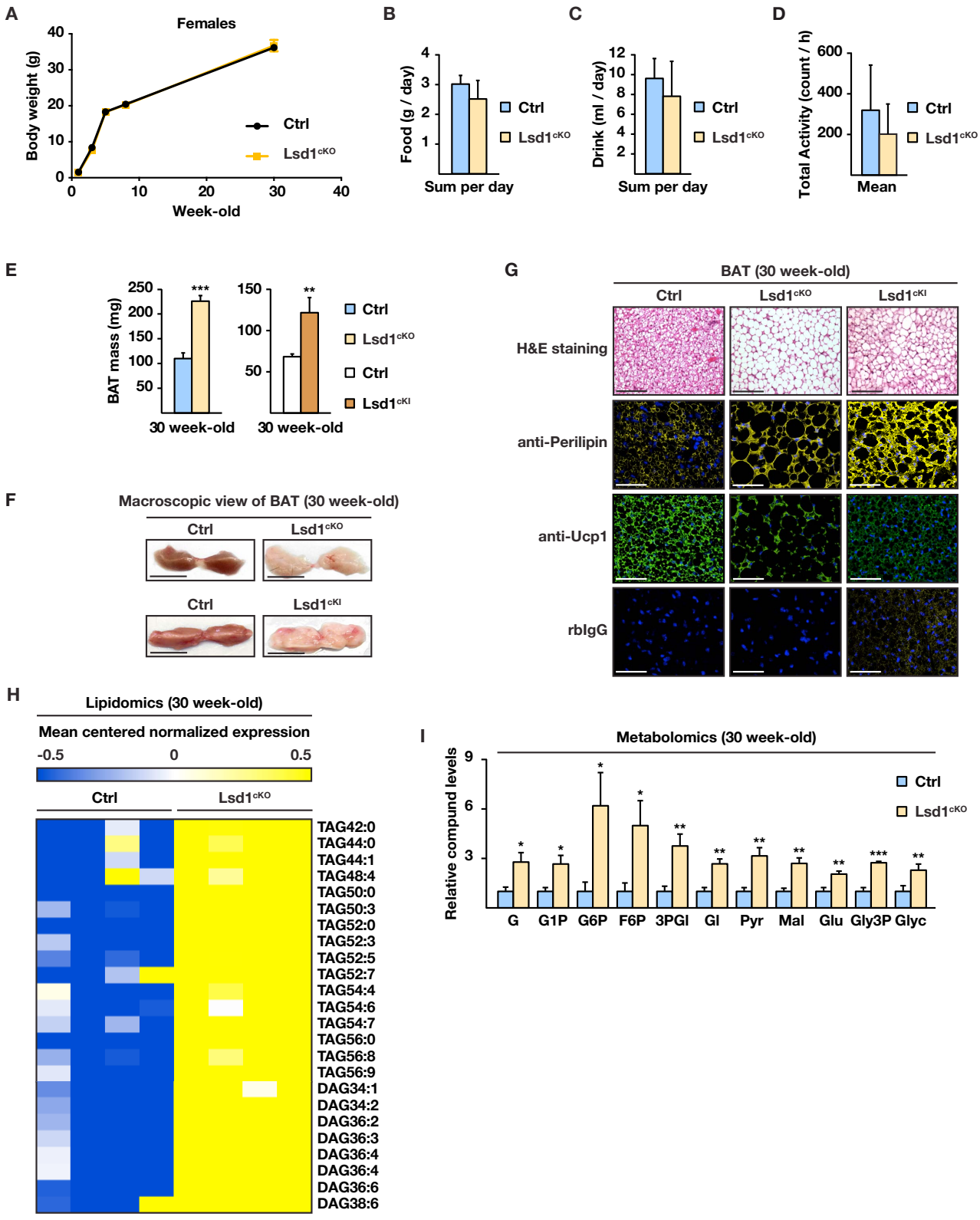
A
Females
Body weight (g)
Week-old
Ctrl
Lsd1cKO
B
Food (g / day)
Sum per day
C
Drink (ml / day)
Sum per day
D
Total Activity (count / h)
Mean
E
BAT mass (mg)
30 week-old
30 week-old
F
Macroscopic view of BAT (30 week-old)
G
BAT (30 week-old)
Lsd1cKI
H&E staining
anti-Perilipin
anti-Ucp1
rbIgG
H
Lipidomics (30 week-old)
Mean centered normalized expression
TAG42:0
TAG44:0
TAG44:1
TAG48:4
TAG50:0
TAG50:3
TAG52:0
TAG52:3
TAG52:5
TAG52:7
TAG54:4
TAG54:6
TAG54:7
TAG56:0
TAG56:8
TAG56:9
DAG34:1
DAG34:2
DAG36:2
DAG36:3
DAG36:4
DAG36:4
DAG36:6
DAG38:6
I
Metabolomics (30 week-old)
Relative compund levels
G
G1P
G6P
F6P
3PGl
Gl
Pyr
Mal
Glu
Gly3P
Glyc

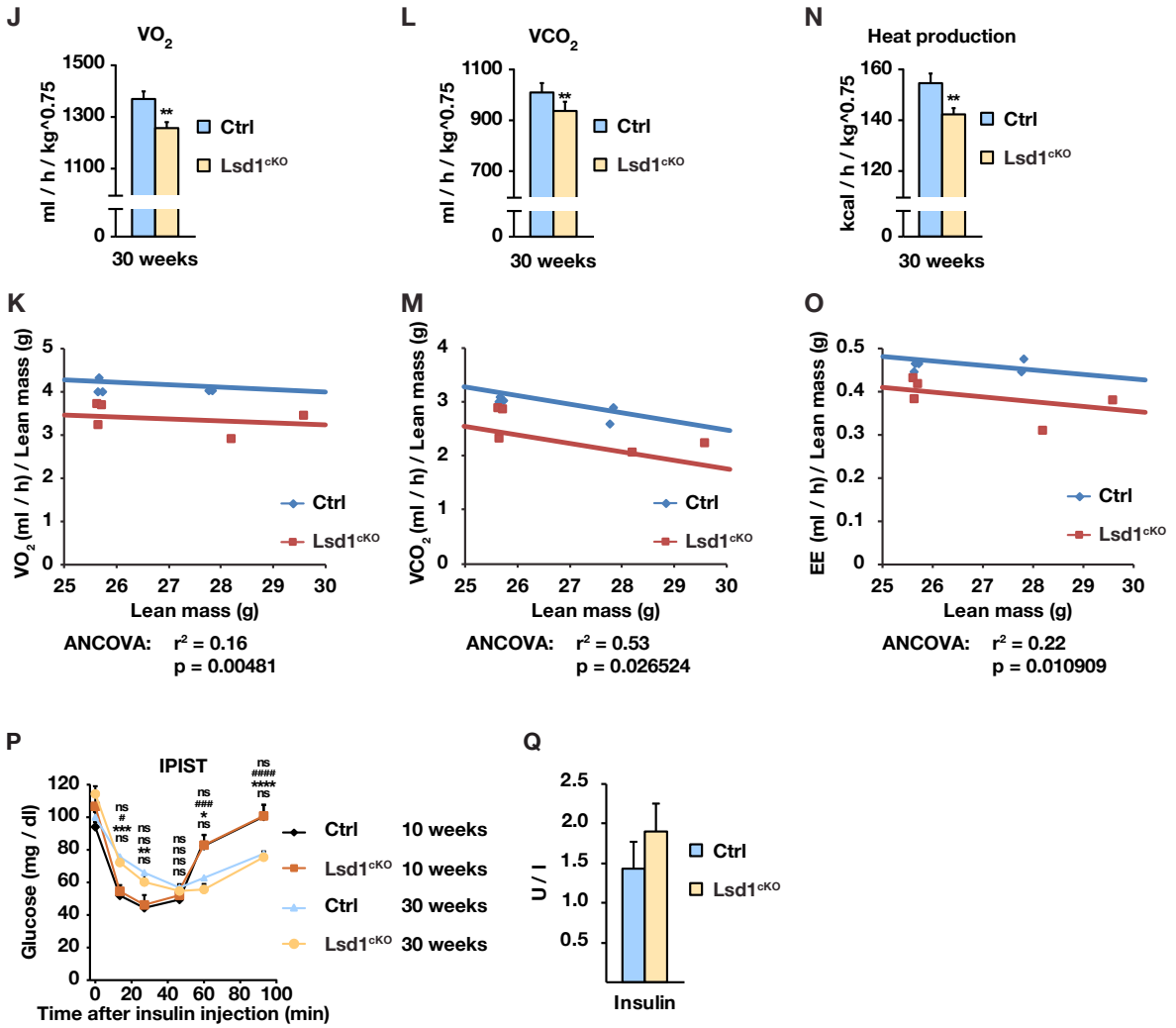

Figure S6 (related to Figure 6). Lsd1^{cKO} mice have a higher glucose uptake despite an increased body weight.
(A) Body weight of control and Lsd1^{cKO} female mice at indicated age (mean + SEM; two-way ANOVA with repeated measures; factor interaction: $p_{genotype/time}$: ns; Ctrl n = 6, Lsd1^{cKO} n = 6).
(B-D) (B) Food consumption, (C) drink consumption, and (D) total activity of 30 week-old control (Ctrl) and Lsd1^{cKO} mice (mean + SEM, Ctrl n = 9, Lsd1^{cKO} n = 7).
(E-F) (E) Mass and (F) macroscopic view of BAT of 30 week-old Ctrl, Lsd1^{cKO}, and Lsd1^{cKI} mice [(D) mean + SEM, **p<0.01, ***p<0.001, Ctrl n = 9, Lsd1^{cKO} n = 7, and Ctrl n = 7, Lsd1^{cKI} n = 6].
(G) H&E staining and perilipin or Ucp1 immunofluorescence of representative sections of BAT of 30 week-old Ctrl, Lsd1^{cKO}, and Lsd1^{cKI} mice. Nuclei were counterstained with DAPI. Rabbit IgG (rbIgG) was used as negative control.
(H) Lipidomic analysis of BAT from 30 week-old Ctrl and Lsd1^{cKO} mice (mean + SEM, n = 5).
(I) Relative abundance of indicated metabolites in BAT of Ctrl and Lsd1^{cKO} mice. G: glucose, G1P: glucose-1-phosphate, G6P: glucose-6-phosphate, F6P: fructose-6-phosphate, 3PGl: 3-phosphoglycerate, Gl: glycerate, Pyr: pyruvate, Mal: malate, Glu: glutamate, Gly3P: glycerol-3-phosphate, Glyc: glycerol (mean + SEM, n = 5, *p<0.05, **p<0.01, ***p<0.001).
(J-O) (J-K) VO_2, (L-M) VCO_2, and (N-O) energy expenditure of 30 week-old control and Lsd1^{cKO} mice represented related to the metabolic body weight (J, L, and N) (mean + SEM, *p<0.05, **p<0.01, Ctrl n = 8, Lsd1^{cKO} n = 7) or as a linear regression (K, M, and O) for which an ANCOVA analysis was performed.
(P) Intraperitoneal insulin sensitive test (IPIST) for 10 week-old or 30 week-old control and Lsd1^{cKO} mice starved for 6 hours prior to analysis (mean + SEM, two-way ANOVA, Ctrl 10 week-old vs Lsd1^{cKO} 10 week-old: ns p>0.05; Ctrl 10 week-old vs Ctrl 30 week-old: **p<0.01, ***p<0.001, ****p<0.0001; Lsd1^{cKO} 10 week-old vs Lsd1^{cKO} 30 week-old: # p<0.05, ### p<0.001, #### p<0.0001; Ctrl 30 week-old vs Lsd1^{cKO} 30 week-old: ns p>0.05; Ctrl n = 8, Lsd1^{cKO} n = 7).
(Q) Serum insulin levels of 30 week-old control (Ctrl) and Lsd1^{cKO} mice (mean + SEM, Ctrl n = 9, Lsd1^{cKO} n = 7).
Scale bars: (F) 7 mm, (G) H&E staining 100 µm, immunofluorescence 20 µm.

Supplemental Tables

Table S1 (related to Figure 1). mRNA ratios [represented as log(fold change), logFC] for BAT- (yellow) and WAT-selective (bleu) genes in BAT and WAT of 10 week-old control mice (BAT / WAT) and in BAT of 10 week-old Lsd1^{cKO} and control mice (cKO / Ctrl).

Table S2 (related to Figure 3). List of the 163 Lsd1 interacting proteins identified by immunoprecipitation followed by mass-spectrometry. The calculation of log2-value is described in Materials and Methods.

Gene	Sense	Primer 5'-3'
***Lsd1* WT/L2**	fw	CCTCAGTAGGCCTGGTTTGT
***Lsd1* WT/L2**	rev	TTGGTTTTGGTTGACCCTTC
***Lsd1* L-**	fw	CCGTGGAAATTCGTGCACTC
***Lsd1* L-**	rev	GCAGGCGGTTTGAAATGTATTC
***Lsd1* WT/KI**	fw	CCAGCTGCTTGTTGGTGC
***Lsd1* WT/KI**	rev	TGGAGTGAAGTGGTTACCTGC
Ucp1-Cre	fw	CCTCTGCACTGGCACTACCT
Ucp1-Cre	rev	TCTTCTTCTTGGGCACCATC

Table S3 (related to Figure S1). Primers used for genotyping

Gene	Sense	Primer 5'-3'
Tbp	fw	GAAGCTGCGGTACAATTCCAG
Tbp	rev	CCCCTTGTACCCTTCACCAAT
36b4	fw	GCGTCCTGGCATTGTCTGT
36b4	rev	GCAAATGCAGATGGATCAGCC
Hprt	fw	AGGGCATATCCAACAACAAACTT
Hprt	rev	GTTAAGCAGTACAGCCCCAAA
Lsd1	fw	GTGTTCTGGGACCCAAGTGT
Lsd1	rev	TAATGCCAGCAGCTTCTCCT
Bmp4	fw	GCTGGAATGATTGGATTGTGG
Bmp4	rev	ATGGCATGGTTGGTTGAGTTG
Egfr	fw	ACACTGCTGGTGTTGCTGAC
Egfr	rev	CCCAAGGACCACTTCACAGT
Pdk3	fw	TTTGAGAGGCTGCCAGTTTT
Pdk3	rev	CGTCTCTGGTTGACTTGCAG
Fads1	fw	AAGGCCAACCACCTCTTCTT
Fads1	rev	ACTGACAGGTGCCCAAAGTC
Apoe	fw	GGTTCGAGCCAATAGTGGAA
Apoe	rev	TATTAAGCAAGGGCCACCAG
Klhl13	fw	AGAATTGGTTGCTGCAATACTCC
Klhl13	rev	AAGGCACAGTTTCAAGTGCTG
Rtn1	fw	TCCGCATCTACAAGTCCGTT
Rtn1	rev	AAAAGCCTCCGTAGCTCCTT
Bmp1	fw	CAAGGCCCACTTCTTCTCAG
Bmp1	rev	TTGTGTTCACAGCCAGCTTC
Wls	fw	ATTTGACTGGACCTGGATGC
Wls	rev	TTCCAGTACCCTGCAATGTG
Ucp1	fw	TGGCAAAAACAGAAGGATT
Ucp1	rev	CGAGTCGCAGAAAAGAAGC
Slc27a2	fw	ATGCCGTGTCCGTCTTTTAC
Slc27a2	rev	CGATGATGATTGATGGTTGC
Acadm	fw	GGATGACGGAGCAGCCAATG
Acadm	rev	ATACTCGTCACCCTTCTTCT
Oplah	fw	CTTCACGCACGTCTCCTTGT
Oplah	rev	GCATCTGCACAGGCCGTAT
Acadl	fw	TTGGTGGGGACTTGCTCTCA
Acadl	rev	CTGTTCTTTTGTGCCGTAAT
Cox6a1	fw	TGCTCAACGTGTTCCTCAAG
Cox6a1	rev	TAAGGGTCCAAAACCAGTGC
Prdm16	fw	CCCCCAACGCTCTCGGATCC
Prdm16	rev	CCGAAGCAGCGGTTGCACAG
Cox17	fw	ATAGTTGCTTTCGCCTGGAA
Cox17	rev	ACAAAGTAGGCCACCACGTC
Elovl1	fw	TTCCAACTTCGAGGCTTCAT
Elovl1	rev	GCTCAATGACCTTGGAAAGC
Elovl4	fw	ACTATGGGCTGACTGCGTTC
Elovl4	rev	TTCCGGTTTTTGACTGCTTC
Elovl7	fw	TCATCCTGGGCCTCTATGTC
Elovl7	rev	ACCATCCTCATTGCTCTTGG
Fads2	fw	GCTCTCAGATCACCGAGGAC
Fads2	rev	AGTGCCGAAGTACGAGAGGA

Gene	Sense	Primer 5'-3'
Hk1	fw	TGGACAAAGGGATTCAAAGC
Hk1	rev	CTCCACCATCTCCACGTTTT
Pfkm	fw	GCTGTGGTCCGAGTTGGTAT
Pfkm	rev	CTCTCGGAAGTCCTTGCATC
Fbp1	fw	CCATCATAATCGAACCTGAG
Fbp1	rev	CTTCTCAGAAGGCTCATCAG
Aldoc	fw	CTGCTCAAGCCCAATATGGT
Aldoc	rev	CTTCACTCTGACCCCCAGAC
Pgam2	fw	ACACCTCCATCAGCAAGGAC
Pgam2	rev	GGGCTGCAATAAGCACTCTC
Eno3	fw	CTCCGAGATGGAGACAAAGC
Eno3	rev	CGTCCAGCTCAATCATGAAC
Ldha	fw	AGACAAACTCAAGGGCGAGA
Ldha	rev	CAGCTTGCAGTGTGGACTGT
Mpc1	fw	ACTTTCGCCCTCTGTTGCTA
Mpc1	rev	AAGTCGTCCTCCCTGAATGA
Mpc2	fw	TGTTGCTGCCAAAGAAATTG
Mpc2	rev	GCTAGTCCAGCACACACCAA
Dlat	fw	TCCAAAGCGAGAGAGGGTAA
Dlat	rev	AGCACCGATTGCCAGAATAC
Pdhx	fw	ATTCCCAAGGATGTCAGTGC
Pdhx	rev	CAGCTGGACTTAAGCGGAAC
Got1	fw	GCTGACTTCTTAGGGCGATG
Got1	rev	TAGCAATAGGGCCGAATGTC
Got2	fw	TTGATCCGTCCCCTGTATTC
Got2	rev	TTAGGCCGGTGAAACAGAAC
Pck2	Fw	GGGGTACCACTGGTGTACGA
Pck2	rev	TCTCTCCGGAACCAATTGAC
Glut1	fw	TCAACACGGCCTTCACTG
Glut1	rev	CACGATGCTCAGATAGGACATC
Glut3	fw	TTCTGGTCGGAATGCTCTTC
Glut3	rev	AATGTCCTCGAAAGTCCTGC
Glut12	fw	ACTATCCCAGCAACCCTCCT
Glut12	rev	AAACTCCTCCAGGGACTGGT
Ndufa6	fw	GTCACAGACCCCAGAGTGGT
Ndufa6	rev	TAACATGCACCTTCCCATCA
Sdha	fw	ACACAGACCTGGTGGAGACC
Sdha	rev	GGATGGGCTTGGAGTAATCA
Uqcrc1	fw	GACAACGTGACCCTCCAAGT
Uqcrc1	rev	ACTGGTACATAGGCGCATCC
Cox8b	fw	GAACCATGAAGCCAACGACT
Cox8b	rev	GCGAAGTTCACAGTGGTTCC
Atp5b	fw	GAGGGATTACCACCCATCCT
Atp5b	rev	CATGATTCTGCCCAAGGTCT
Cpt1b	fw	CAGCTGGCTGGTTGTTGTCA
Cpt1b	rev	TTGTCGGAAGAAGAAAATGC
Pgc1a	fw	AAGTGTGGAACTCTCTGGAACTG
Pgc1a	rev	GGGTTATCTTGGTTGGCTTTATG
Cox2	fw	CAGTCCCCTCCCTAGGACTT
Cox2	rev	TTTCAGAGCATTGGCCATAGAA
Fasn	fw	AGGATATGGAGAGGGCTGGT
Fasn	rev	ACCCAAGCATCATTTTCGTC

Table S4. Primers used for qPCR analysis

Gene	Sense	Primer 5'-3'
Acadm	fw	CTTCGTGTTGTGCCTGTGTT
Acadm	rev	GCCACTTCTCTCCAGTCACC
Oplah	fw	CAGGGGGAAAGTAGGAAAGG
Oplah	rev	CCAGGCTTGTGTGTCTGTGT
Cox6a1	fw	TTGCGAGCTTTTCTGGTTTT
Cox6a1	rev	GGGCACAACGGAAGAGAATA
Unrelated1	fw	AATGCCTCTCACGCTCAACT
Unrelated1	rev	AAGTGTGTGCCATCCTTTCC
Pdk3	fw	TTCCTTAAAGCCCCGGTAAC
Pdk3	rev	GGGAGGTCTAGAGCCCCTAA
Fads1	fw	ACGGTGAGAGCGGACAATAG
Fads1	rev	ATCCAACCCATGCTTGAGAC
Bmp1	fw	GTCTCTGTCGCTGTCCTTCC
Bmp1	rev	TTCTCAGCTCGGCTTCTAGC
Wls	fw	CTGGCTGTGGCTTGTGTAAA
Wls	rev	GGACAAGAGGCAAAAGCAAC
Unrelated2	fw	AGCCAGGGCTACACAGAGAA
Unrelated2	rev	AGATTCCTGCACCAAAGTGG
Slc2a1	fw	ATCAGAAAGGGACACGGATG
Slc2a1	rev	AAATCCTCCCGAGGAAAGAA
Slc2a12	fw	CTAGACCCAAATCCCGTTGA
Slc2a12	rev	CGCCGAAGAGGAACATTTTA
Hk1	fw	AAACTAGGCGGCTTCACAGA
Hk1	rev	GGGGACCATGAGCTCTTACA
Eno3	fw	GCGGAGAGAGTTACCGAGTG
Eno3	rev	TTCCTGCGTGAAGCCTAAGT
Got1	fw	CCGCAGTGAGCTTAAAGACC
Got1	rev	AGTCGGAAGGTTGTGATTGG
Got2	fw	GTAAGACGGCAGTGGATGGT
Got2	rev	CTTGCGAGTTTCCATGACCT
Elovl1	fw	CAGCCCTTAGTAGGCACAGC
Elovl1	rev	CACCCAGCTTCTTCTTGAGG

Table S5. Primers used for ChIP-qPCR analysis

Supplemental Experimental Procedures

Generation of conditional *Lsd1* knock-out and knock-in mice

All experiments were performed in C57/Bl6N background. The targeting strategy for the conditional deletion of the first exon of *Lsd1* (*Lsd1*^{tm1Schüle}) is available upon request (Zhu et al., 2014). Briefly, conditional *Lsd1* mice were mated with *Ucp1-Cre* mice to selectively ablate *Lsd1* in brown adipose tissue (Figures S1A and S1B). Homozygous conditional mice were used as controls. Mice were genotyped with primers for detection of conditional *Lsd1* alleles and *Cre* recombinase (Table S3).

Lsd1 knock-in (KI) mice were generated by Taconic [C57BL/6-Kdm1a$^{tm2931(K662A,\ W752A,\ Y762S)Arte}$]. The targeting vector has been engineered as follows (Figure S1F). Wild-type *Lsd1* exons 15 to 19, including the complete 3' untranslated region (UTR), were flanked by *loxP* sites. An additional polyadenylation signal (hGHpA: human Growth Hormone polyadenylation signal) was inserted between the 3' UTR and the distal *loxP* site in order to prevent downstream transcription of the mutated *Lsd1* exons 15 to 19. The size of the *loxP*-flanked region is 5.1 kb. Exons 15 to 19, including the splice acceptor site of intron 14, were duplicated and inserted downstream of the distal *loxP* site. Intron 15 was removed from the wild-type and the duplicated region in order to create a fusion of exon 15/16. K662A mutation was introduced into the duplicated exon 15, W752A and Y762S mutations were introduced into the duplicated exon 18. A second hGHpA cassette was inserted downstream of the duplicated 3' UTR. Positive selection markers were flanked by *FRT* (Neomycin resistance) and *F3* (Puromycin resistance) sites, and inserted into intron 14 and downstream of the second hGHpA, respectively. The targeting vector has been generated using BAC clones from the C57BL/6J RPCIB-731 BAC library and transfected into the Taconic Artemis C57BL/6N Tac ES cell line. Homologous recombinant clones were isolated using double positive (NeoR and PuroR) selection (in order to increase the efficiency of co-integration of both *loxP* sites and the point mutations). The conditional KI allele was obtained after Flp-mediated deletion of the selection markers. This allele expresses wild-type Lsd1 protein. The presence of the first hGHpA cassette downstream of the wild-type exon 19 should prevent transcription of the mutated exons 15 to 19. Conditional *Lsd1*$^{KI/KI}$ mice were crossed to *Ucp1-Cre* mice to selectively express mutated Lsd1 in brown adipose tissue (Lsd1^{cKI} mice). Homozygous conditional *Lsd1*$^{KI/KI}$ mice were used as controls. Mice were genotyped with primers for detection of conditional KI alleles and *Cre recombinase* (Figure S1G and Table S3).

RNA preparation, qRT-PCR, and RNA sequencing (RNA-seq)

RNA was isolated with TRIzol Reagent (Invitrogen) and processed as described (Duteil et al., 2014). Data were analyzed using the standard curve method (Bookout et al., 2006). *36b4*, *Hprt*, or *β-actin* were used for normalization. Primer sequences are given in Table S4.

RNA samples were sequenced by the standard Illumina protocol to create raw sequence files (.fastq files). We annotated these reads to the mm10 build of the mouse genome using TopHat version 2. The aligned reads were counted with the homer software (analyze RNA) and DEGs were identified using EdgeR and DESeq version 1.8.3. Differentially regulated genes (reads > 50, $p < 0.01$) were further used for pathway analysis in WebGestalt (Heinz et al., 2010; Wang et al., 2013).

Protein analyses

Western blot analysis, co-immunoprecipitation assays, gel filtration, and mass spectrometry experiments were performed as described (Duteil et al., 2014; Metzger et al., 2016). For gel filtration, brown adipocytes were harvested and suspended in isolation buffer (10 mM HEPES-KOH, pH 7.9, 1.5 mM $MgCl_2$, 10 mM KCl, 0.5 mM DTT, and complete protease inhibitor cocktail, Roche), allowed to swell on ice for 10 min, and pelleted. Isolated nuclei were resuspended in 20 mM HEPES-KOH, pH 7.9, 25 % glycerol, 420 mM NaCl, 1.5 mM $MgCl_2$, 0.2 mM EDTA, 0.5 mM DTT, and complete protease inhibitor cocktail, incubated on ice for 20 min and centrifuged at 14,000 r.p.m. for 10 min. Nuclear complexes were separated by gel filtration on a Superose 6^{TM} 10/300 GL column (GE Healthcare) using the ÄKTA pure 25 system (GE Healthcare). The void volume was 7.2 mL. 60 fractions of 300 µL were collected from an elution volume of 4.8 mL. The gel filtration buffer was composed of 50 mM KCl, 50 mM $NaCH_3COOH$, pH 7.2 including protease inhibitors and phosphatase inhibitors (Roche Diagnostics). Column calibration was done using carbonic anhydrase (26 kDa), bovin serum albumin (66 kDa), alchol dehydrogenase (150 kDa), ☆-amylase (200 kDa), apoferritin (443 kDa), and thyroglobulin (669 kDa) as markers according to the method provided by the supplier. Western blot membranes were decorated using following antibodies: anti-Lsd1 [3544 , Schüle laboratory (Duteil et al., 2014), 1/1000], anti-Ucp1 (Abcam, ab10983, 1/1000), anti-Apoe (Santa Cruz, M-20, 1/200), anti-Nrf1 (Abcam, ab55744, 1/500), anti-Hdac1 (Abcam, ab7028-50, 1/1000), anti-Hdac2 (Santa Cruz, sc-7899, 1/2500), anti-Rcor1 (Abcam, ab32631, 1/400), anti-Rcor3 (Abcam, ab76921, 1/2000), anti-Arid1a (Santa Cruz, sc-373784, 1/200), anti-phosphoAcc (Cell signaling, 11818, 1/1000), anti-Acc (Cell signaling, 3676, 1/1000), anti-β-Tubulin (Sigma, T6074, 1/10000), and anti-β-Actin (Sigma, A1978, 1/10000). Secondary antibodies conjugated to horseradish peroxidase (GE Healthcare) were detected using an enhanced chemiluminescence detection system (GE Healthcare). For immunoprecipitation assay, 500 mg of

protein extracts were incubated with 5 µg of anti-Lsd1 (Sigma, L-4481) and processed as described (Metzger et al., 2010). Mass spectrometry experiments were performed as described (Metzger et al., 2016). Lsd1 antibodies used for immunoprecipitation were Sigma L-4481 (Ab3 in Figure S3F), and the two Lsd1 antibodies 20752 and 3544 (Ab1 and Ab2 in Figure S3F, respectively) that we previously characterized (Duteil et al., 2014). The number of peptides obtained for each protein after Lsd1 immunoprecipitation was subtracted from the number of peptides obtained with IgG. The resulting number was then normalized to the number of Lsd1 peptides on a log2 basis. The calculation of log2-value is presented in Table S2. GO cellular component analysis was performed using the Panther algorithm (Ashburner et al., 2000).

Primary cell isolation and cell culture

BAT was cut in small pieces and incubated with 2 mg/ml collagenase I (CLS-1, Worthington) for 45 min. The cell suspension was filtered through a 150 µm nylon mesh and the stromal-vascular fraction (SVF) was isolated by low-speed centrifugation. For FACS analysis, the erythrocyte-free SVF was incubated with a mix of antibodies against different surface markers as described previously (Duteil et al., 2014; Wu et al., 2012) and sorted using an Aria flow cytometer (BD Biosciences). Dead cells were removed using DAPI staining (1/10000). Primary adipocytes were cultured in DMEM High Glucose containing 20 % fetal calf serum (FCS) and 2 % of 1 M Hepes buffer in dishes coated with collagen. Alternatively, preiBA cells were cultured in DMEM containing sodium pyruvate and glutamine (GIBCO 11995-065) supplemented with 10 % FCS. Differentiation of primary adipocytes and preiBA cells was induced by treatment of confluent cells with an adipogenic mixture consisting of 850 nM insulin (Gibco), 1 µM dexamethasone (Calbiochem), 1 µM rosiglitazone (Cayman), 125 nM indomethacin (Sigma), 1 nM T3 (Sigma), and 500 µM isobutylmethylxanthine (Serva) in the presence of 10 % FCS. The differentiation medium was replaced 2 days later with medium supplemented with 10 % FCS, 850 nM insulin, and 1 nM T3 for 2 days. Subsequently, cells were cultured in the same medium for 4 more days and considered as differentiated. Differentiated cells were transfected with 1 mM siRNA against Lsd1, Nrf1, Rcor1, Rcor3, or unrelated control (Invitrogen) using Lipofectamine RNAimax (Invitrogen) according to the manufacturer's instructions. siRNA oligonucleotide sequences were as follows:
Lsd1 siRNA: 5'-CCCAAAGAUCCAGCUGACGUUUGAA-3';
Nrf1 siRNA: 5'-UAUGGUAGCCAUGUGUUCAGUUUGG-3';
Rcor1 siRNA: 5'-GCGCAGUCAAGAACGAGACAAUCUU-3';
Rcor3 siRNA: 5'-UCCCAGAUGCCAAAUUGGAUGAAUA-3';
unrelated control siRNA: 5'-UUCUUAGCAAGACUGGUCUCUAGGG-3'.
Lsd1 inhibitor QC6688 was applied to differentiated cells at 100 nM (in EtOH) for 3 days. EtOH was used as a vehicle. Brown adipocytes were either harvested and snap-frozen for RNA, protein, and chromatin immunoprecipitation experiments, fixed for 1 h with 4 % PFA and stained with Oil Red O, or fixed for 5 min with 1 % PFA for chromatin immunoprecipitation experiments (see bellow).

Chromatin immunoprecipitation (ChIP) and ChIP sequencing (ChIP-seq)

Chromatin immunoprecipitation experiments were performed using anti-Lsd1 (20752, Schüle laboratory), anti-Nrf1 (Abcam, ab55744), anti-Rcor1 (Abcam, ab32631), anti-Rcor3 (Abcam, ab76921), H3K9me2 (Diagenode, Mab-154-050), or H3K4me2 (Diagenode, CS-035-100) antibodies, or a rabbit IgG negative control on protein G-Sepharose 4B (GE Healthcare) essentially as described (Metzger et al., 2008). For ChIP experiments, ChIPed DNA was processed by qPCR analyses with the primers described in Table S5. For ChIP-seq analysis, libraries were prepared from Lsd1-immunoprecipitated DNA according to standard methods. ChIP-seq libraries were sequenced using a HiSeq 2000 (Illumina) and mapped to the mm10 reference genome using bowtie 2 (Langmead et al., 2009). Data were analyzed using the peak finding algorithm MACS 1.41 (Zhang et al., 2008) using input as control. All peaks with a FDR greater than 0.3 % were excluded from further analysis. The uniquely mapped reads were used to generate the genome-wide intensity profiles, which were visualized using the IGV genome browser (Thorvaldsdottir et al., 2012). HOMER (Heinz et al., 2010) was used to annotate peaks, to calculate overlaps between different peak files, and for motif searches. The genomic features (promoter, exon, intron, 3' UTR, and intergenic regions) were defined and calculated using Refseq and HOMER.

Histological and immunofluorescence analysis

Tissues were fixed in 10 % buffered formalin and embedded in paraffin. 5 µm paraffin sections were deparaffinised and rehydrated. Hematoxylin and eosin staining was performed as described (Duteil et al., 2014). For immunofluorescence analyses, rehydrated sections were boiled in antigen unmasking solution (Tris buffer pH 9) for 20 min, cooled to room temperature, washed 3 times with PBS, 0.1 % Triton-X100 for 5 min, blocked for 1 h in 5 % FBS (Gibco, 10270-106) in PBS, 0.1 % Triton-X100, and incubated overnight at 4°C with anti-Lsd1 (1/1000), anti-Ucp1 (Abcam, ab10983, 1/500), or anti-Perilipin (Abcam, ab3526, 1/400) antibodies. Slides were then incubated with secondary antibody conjugated to Alexa488 (Invitrogen, 1/400) and mounted in aqueous

medium (Fluoromount-G, SouthernBiotech, 0100-01) with DAPI (Sigma, D-9542, 1/1000). Ultrastructural analyses were performed as described (Duteil et al., 2014).

Measuring activities of metabolic enzymes

Glucose uptake, hexokinase, phosphofructokinase, enolase, lactate dehydrogenase, glutamate oxaloacetic transaminase, NAD^+/NADH ratio, hormone-sensitive lipase, LPL, and fatty acid synthase activities were assessed by the Glucose Uptake Assay Kit (ab136955, abcam), Hexokinase Colorimetric Assay Kit (MAK091, Sigma), the Phosphofructokinase Colorimetric Assay Kit (MAK093, Sigma), the Enolase Activity Colorimetric/Fluorometric Assay Kit (K691-100, Bio Vision), the Lactate Dehydrogenase Activity Assay Kit (Sigma, MAK066), the Glutamate-oxaloacetate transaminase kit (K753-100, Bio Vision), the NAD/NADH Assay Kit (ab65348, abcam), the Lipase Activity Assay Kit (MAK046, Sigma), the LPL Activity Assay kit (MAK109, Sigma), and Fatty Acid Synthase ELISA kit (ABIN425666, antibodies-online), respectively. All activities were measured using 20-50 mg of BAT according to the manufacturer recommendations.

Metabolomic and lipidomic analyses

Tissue samples were grinded with a Retsch MM440 instrument and further extracted as described in (Giavalisco et al., 2009). LC-MS measurements were performed using a Waters ACQUITY UPLC system coupled to a Thermo-Fisher QExactive mass spectrometer. Lipophilic compounds were separated using a C8 and hydrophilic compounds using a C18 reverse phase column, respectively. The mobile phase composition and electrospray parameters are described in (Giavalisco et al., 2009). Chromatograms were recorded in survey MS mode (Mass Range [100 - 1500]) for hydrophilic compounds and in DDA MS/MS (40 eV collision energy) mode for lipophilic compounds. GC-MS measurements were performed as follows. An aliquot of lower polar extraction phase was dried and the dry residue was sequentially derivatized by methoxyamine/MSTFA and injected onto DB35 GC column (Agilent Technologies GC machine) coupled to Leco Pegasus HT mass spectrometer with EI ionization source. Gas elution was performed for two minutes at 85 °C with a further temperature gradient of 15 °C per minute untill a final temperature of 360 °C was reached.

Peak-picking and background removal of the LC-MS data from measurements of hydrophilic extraction phase was accomplished with the Genedata REFINER MS® 7.5 software. Chromatogram alignment and filtering were completed using in-house R-based software. Filtering included removal of isotopic peaks, in-source fragments, and additional lower intense adducts of the same analyte. The annotation of the content of the sample was accomplished by matching the extracted data from the chromatograms with our library of reference compounds in terms of accurate mass and retention time, and the most abundant adduct was used for relative quantification of a metabolite. For GC-MS data of the same extraction phase NetCDF files were exported from the Leco Pegasus software to "R". The package TargetSearch was used to transform retention time to retention index (RI), to align the chromatograms, extract the peaks, and annotate them by comparing the spectra and the RI to the Golm metabolome database. A unique mass was used to relatively quantify each identified metabolite. For those metabolites, which were annotated in both GC-MS and LC-MS data the value with smallest deviation was kept.

Peak-picking of the LC-MS/MS data from measurements of the lipophilic extraction phase was accomplished with the Genedata REFINER MS® 7.5 software without alignment. Identification of lipid species was performed using output.mgf files with dedicated in-house R-based software. Acyl composition of di- and triacylglycerols was established from the [Acyl + NH4] neutral loss in positive ion mode using a pre-formed library of accurate masses for all possible precursor and fragment peaks.

Mitochondrial respiration

10 mg (wet weight) of BAT were minced and incubated in Mir05 with 50 µg/mL Saponin for 30 min at 37 °C to permeabilize the cell membrane. Mir05 is composed of 0.5 mM EGTA, 3 mM $MgCl_2$, 60 mM K-lactobionate, 20 mM Taurine, 10 mM KH_2PO_4, 20 mM HEPES, 110 mM Sucrose, and 1 g/L BSA fatty acid free. Respiration of permeabilized brown adipocytes was measured by high-resolution respiratory using Oxygraph-2K (OROBOROS INSTRUMENTS, Innsburk, Austria) at 37 °C in 2 mL glass chambers. For each experiment, one control mouse and one $Lsd1^{cKO}$ mouse were processed in parallel in the 2 chambers. Mitochondrial respiration was assessed in Mir05 buffer supplemented with 5 mM glutamate and 2 mM malate substrates to activate mitochondrial complex I. After stabilization of mitochondrial respiration, 10 mM succinate were added to activate complex II. Maximal respiration rate was then recorded. 0.5 µM rotenone were finally added to inactivate mitochondrial complex I and measure complex II specific activity. Respiration rates were expressed in pmol / s and reported to 1 mg of tissue. Results presented correspond to maximal mitochondrial respiration rate. Alternatively, mitochondrial respiration was analyzed using 100 µM palmitoyl-L-carnitin as substrate.

Supplemental References

Ashburner, M., Ball, C.A., Blake, J.A., Botstein, D., Butler, H., Cherry, J.M., Davis, A.P., Dolinski, K., Dwight, S.S., Eppig, J.T.*, et al.* (2000). Gene ontology: tool for the unification of biology. The Gene Ontology Consortium. Nat Genet *25*, 25-29.

Bookout, A.L., Cummins, C.L., Mangelsdorf, D.J., Pesola, J.M., and Kramer, M.F. (2006). High-throughput real-time quantitative reverse transcription PCR. Curr Protoc Mol Biol *Chapter 15*, Unit 15 18.

Duteil, D., Metzger, E., Willmann, D., Karagianni, P., Friedrichs, N., Greschik, H., Gunther, T., Buettner, R., Talianidis, I., Metzger, D.*, et al.* (2014). LSD1 promotes oxidative metabolism of white adipose tissue. Nat Commun *5*, 4093.

Giavalisco, P., Kohl, K., Hummel, J., Seiwert, B., and Willmitzer, L. (2009). 13C isotope-labeled metabolomes allowing for improved compound annotation and relative quantification in liquid chromatography-mass spectrometry-based metabolomic research. Anal Chem *81*, 6546-6551.

Heinz, S., Benner, C., Spann, N., Bertolino, E., Lin, Y.C., Laslo, P., Cheng, J.X., Murre, C., Singh, H., and Glass, C.K. (2010). Simple combinations of lineage-determining transcription factors prime cis-regulatory elements required for macrophage and B cell identities. Mol Cell *38*, 576-589.

Langmead, B., Trapnell, C., Pop, M., and Salzberg, S.L. (2009). Ultrafast and memory-efficient alignment of short DNA sequences to the human genome. Genome Biol *10*, R25.

Metzger, E., Imhof, A., Patel, D., Kahl, P., Hoffmeyer, K., Friedrichs, N., Müller, J.M., Greschik, H., Kirfel, J., Ji, S.*, et al.* (2010). Phosphorylation of histone H3T6 by PKCbeta(I) controls demethylation at histone H3K4. Nature *464*, 792-796.

Metzger, E., Willmann, D., McMillan, J., Forne, I., Metzger, P., Gerhardt, S., Petroll, K., von Maessenhausen, A., Urban, S., Schott, A.K.*, et al.* (2016). Assembly of methylated KDM1A and CHD1 drives androgen receptor-dependent transcription and translocation. Nat Struct Mol Biol *23*, 132-139.

Metzger, E., Yin, N., Wissmann, M., Kunowska, N., Fischer, K., Friedrichs, N., Patnaik, D., Higgins, J.M., Potier, N., Scheidtmann, K.H.*, et al.* (2008). Phosphorylation of histone H3 at threonine 11 establishes a novel chromatin mark for transcriptional regulation. Nat Cell Biol *10*, 53-60.

Thorvaldsdottir, H., Robinson, J.T., and Mesirov, J.P. (2012). Integrative Genomics Viewer (IGV): high-performance genomics data visualization and exploration. Brief Bioinform.

Wang, J., Duncan, D., Shi, Z., and Zhang, B. (2013). WEB-based GEne SeT AnaLysis Toolkit (WebGestalt): update 2013. Nucleic Acids Res *41*, W77-83.

Wu, J., Bostrom, P., Sparks, L.M., Ye, L., Choi, J.H., Giang, A.H., Khandekar, M., Virtanen, K.A., Nuutila, P., Schaart, G.*, et al.* (2012). Beige adipocytes are a distinct type of thermogenic fat cell in mouse and human. Cell *150*, 366-376.

Zhang, Y., Liu, T., Meyer, C.A., Eeckhoute, J., Johnson, D.S., Bernstein, B.E., Nusbaum, C., Myers, R.M., Brown, M., Li, W.*, et al.* (2008). Model-based analysis of ChIP-Seq (MACS). Genome Biol *9*, R137.

Zhu, D., Holz, S., Metzger, E., Pavlovic, M., Jandausch, A., Jilg, C., Galgoczy, P., Herz, C., Moser, M., Metzger, D.*, et al.* (2014). Lysine-specific demethylase 1 regulates differentiation onset and migration of trophoblast stem cells. Nat Commun *5*, 3174.